Structural Durability & Health Monitoring

Tech Science Press

https://doi.org/10.32604/sdhm.2026.079079

ARTICLE

Analysis of Geometric Imperfections in Cold-formed Aluminium Alloy Channel Members

Hieu Nghia Hoang[1], Ngoc Hieu Pham[2,*], Quoc Anh Vu[2] and Trong Nghia Mai[2]

[1]Faculty of Technology and Engineering, Haiphong University, Haiphong, Vietnam
[2]Faculty of Civil Engineering, Hanoi Architectural University, Hanoi, Vietnam

*Corresponding Author: Ngoc Hieu Pham. Email: hieupn@hau.edu.vn

Received: 14 January 2026; Accepted: 17 March 2026; Published: 30 June 2026

ABSTRACT: The paper presents an analysis of measured geometric imperfections in cold-formed aluminium alloy channel members that is the base for the proposal of representative values for each imperfection component for use in future research and design standards. Cold-formed aluminium alloy sections have recently been developed and found to be more cost-effective than conventional extruded sections. Cold-formed metal sections typically contain significant geometric imperfections; the effects of these imperfections have been demonstrated in numerous previous studies and should therefore be considered in analyses. Cold-formed aluminium sections remain relatively new worldwide, and available data on their geometric imperfections are still limited. This study, therefore, compiles measured imperfection data from a national research project on cold-formed aluminium sections. These data are classified according to individual imperfection components, and then representative values are proposed based on section thickness and slenderness. The proposed values are validated through comparison between finite element model predictions and experimental results for cold-formed aluminium alloy channel members. It is found that very good agreement is observed between the two results. The paper also provides coefficients of variation to account for the effects of geometric imperfections on the strength of cold-formed aluminium members. These coefficients can be considered for inclusion in design standards.

KEYWORDS: Analysis; geometric imperfection; cold-formed aluminium alloy; channel members

1 Introduction

Aluminium alloys have become increasingly popular in structural engineering applications due to their desirable mechanical and physical properties [1]. Traditionally, aluminium alloy sections are produced through the extrusion process. BlueScope Permalite in Australia [2] has recently introduced roll-forming as an alternative manufacturing technique for manufacturing channel and zed sections. Compared with extrusion, the roll-forming process offers higher production efficiency, lower costs, and can potentially improve the strength of aluminium alloys. These favourable attributes of cold-formed aluminium sections are expected to stimulate broader interest in global markets.

The stability of cold-formed aluminium sections against buckling is greatly influenced by their geometric imperfections. Geometric imperfections are inevitably introduced into cold-formed members during manufacturing, transportation, and assembly. As thin-walled elements, these members are highly sensitive to various buckling modes that are strongly affected by such imperfections. Incorporating geometric imperfections in the analysis of cold-formed components, therefore, is crucial. They are generally classified

into global and sectional modes, corresponding to different buckling behaviors. Global imperfections consist of flexural components (F_1, F_2) and an initial twist (T), while sectional imperfections refer to the deformation of plate elements, including local (S_1) and distortional (S_2) imperfections, as shown in Fig. 1. The presence of these imperfections causes buckling to develop gradually from pre-buckling through post-buckling, resulting in an indistinct buckling initiation point.

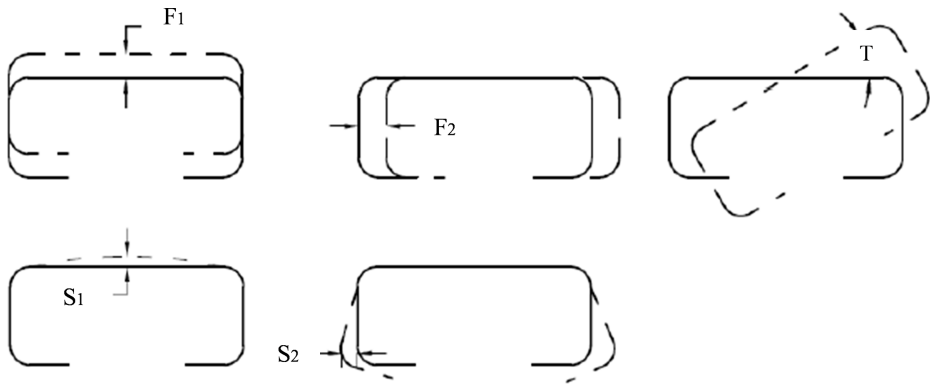

Figure 1: Components of geometric imperfections.

The measurement of geometric imperfections on test specimens is an essential step in such investigations. Numerous techniques have been developed for this purpose, such as displacement transducers [3], optical monitoring systems [4], strain-based sensors [5], 2D and 3D laser scanning technologies [6], and various imaging approaches [7]. The imperfection data, subsequently, are refined and implemented within structural analysis models following the procedure described by Pham et al. [8]. The incorporated imperfections in the analysis model are demonstrated in Fig. 2.

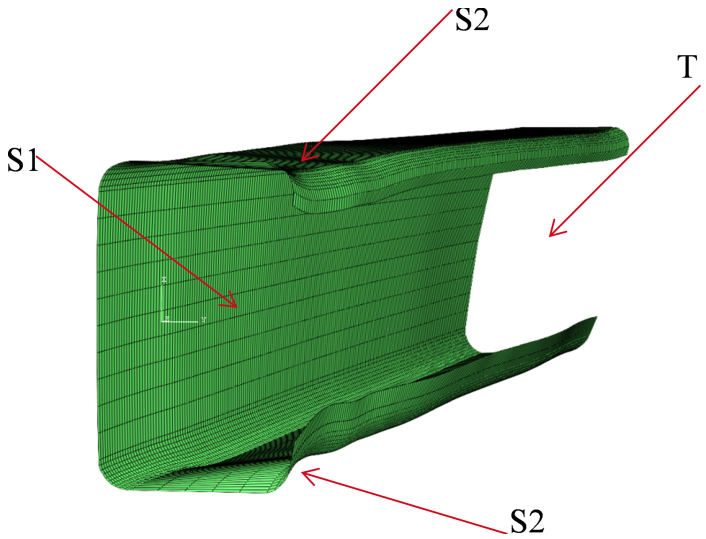

Figure 2: Incorporation of geometric imperfections into the FE model.

A large body of research has focused on understanding how geometric imperfections influence the performance and strength of cold-formed steel members. Many researchers ([9–11]) carried out investigations into the role of torsional imperfections in cold-formed steel channel and zed beams. Their findings showed that the direction of twisting, which originates from the initial torsional imperfection (T), plays a critical role

in determining beam strength. Similarly, Dubina and Ungureanu [12] examined the effects of both the initial twist (T) and flexural imperfections (F_1), concluding that these two global imperfection components have a substantial influence on the flexural strength of structural members. In contrast, sectional imperfections were shown to have minimal effect and could be reasonably neglected.

Borges Dinis et al. [13] later analyzed the individual effects of two sectional imperfection components, (S_1) and (S_2), on the post-buckling response of cold-formed steel channel columns. The findings demonstrated that the (S_2) imperfection component had a pronounced influence on the capacities of the studied sections. Schafer and Zeinoddini [14] focused on the effect of geometric imperfection (S_1) on column strength and proposed corresponding design guidelines. Rzeszut and Garstecki [15] performed a stability evaluation of cold-formed steel sigma columns incorporating both global and local imperfections, showing that overall imperfections reduced the column capacity by approximately 20%, whereas local imperfections caused only a 10% reduction. Furthermore, Schillinger et al. [16] proposed a probabilistic framework for modeling geometric imperfections to investigate the instability of eccentrically loaded I-section columns. In another study, Crisan et al. [17] carried out sensitivity analyses to determine which imperfections most critically influence the compressive strength of perforated steel columns.

Gendy and Hanna [18] explored the influence of geometric imperfections on the ultimate bending moment of cold-formed sigma-section beams. Their findings showed that sectional imperfections in the compression flange have a pronounced impact on the strength of short and medium-span beams, whereas longer beams are predominantly governed by global imperfections. Dou and Pi [19] investigated the influence of global imperfections (F_1) on the capacity of box-section columns by generating random imperfection amplitudes derived from experimental data and incorporating them into analytical simulations to predict capacities. They further proposed unfavorable imperfection components to represent the most detrimental capacity scenarios. Dinis et al. [20] examined the structural response of cold-formed steel channel columns considering both global and sectional imperfections (S_2), and the results were used to identify the most critical imperfection modes for further numerical modeling. Several studies have emphasized that the sensitivity to imperfections differs between beams and columns: sectional imperfections have little to no effect on beam behavior and can generally be neglected [21], whereas they play a more significant role in columns and should be explicitly accounted for in analysis [22–24]. With respect to geometric imperfections in cold-formed aluminium structures, existing research remains scarce, primarily because this structural form is relatively new worldwide.

This paper aims to compile and examine the available experimental data to utilise the measured geometric imperfections of cold-formed aluminium sections for further analysis. The obtained imperfections are then systematically analysed and categorised according to the specific types of imperfections described in the preceding sections. Representative values for each imperfection component are then proposed as functions of sectional slenderness and thickness. These representative values are subsequently incorporated into calibrated finite element (FE) models of cold-formed aluminium members under compression or flexure. The ultimate strengths predicted by these FE models are compared against corresponding experimental results to assess the accuracy and reliability of the proposed representative imperfection values.

A series of numerical analyses will be carried out to evaluate the capacities of cold-formed aluminium alloy members under varying values of global imperfections, in order to account for the influence of geometric imperfections on their strength performance in design. The imperfection amplitudes are generated as random samples derived from the experimental data reported by Pham [25], employing the Latin Hypercube Sampling (LHS) technique [26] to efficiently minimise the number of required simulations. Based on the strength data, coefficients of variation are established and subsequently incorporated into a reliability

assessment of the proposed design formulations using the probability-based Load and Resistance Factor Design (LRFD) approach specified in the American Aluminum Specification [27].

2 Analysis and Clarification of Measured Geometric Imperfections for Cold-Formed Aluminium Alloy Channel Sections

Actual geometric imperfections cannot be directly incorporated in the numerical analyses due to the absence of experimental data; however, representative imperfection parameters can be selected for use in the numerical models. These parameters are established through analytical interpretation of previously measured imperfection data. As illustrated in Fig. 1, measured imperfections are categorized into global and sectional components: (F_1, F_2, T) correspond to bow, camber, and twist, while (S_1, S_2) represent deformations of the web and flange, respectively. The mean value (μ) and standard deviation (σ) are then calculated, and the coefficient of variation is determined as COV = σ/μ. Detailed values of these imperfections are provided in Pham [25] and summarized in Tables 1 and 2.

Table 1: The amplitudes of global imperfection components [25].

Components		F_1/L	F_2/L	T/L (deg/m)
Channel Sections	Mean	1/1580	1/4236	0.599
	St. dev.	1/1973	1/5766	0.607

Table 2: The values of sectional imperfections [25].

Sections		S_1 mm	S_2-flg_1 mm	S_2-flg_2 mm
C10030	Mean	0.284	0.962	0.928
	St. dev.	0.078	0.367	0.361
C25025	Mean	0.739	1.328	1.391
	St. dev.	0.212	0.276	0.309
C40030	Mean	1.366	1.577	1.664
	St. dev.	0.597	0.471	0.669

Note: Channel sections including C10030, C25025 and C40030 were used for the investigation.

Hypothetical imperfections are incorporated for the numerical analyses, encompassing both global and sectional types. Sectional imperfections comprise local and distortional deviations, whereas global imperfections cover flexural and torsional deformations. For each imperfection type, the corresponding geometric deviations are modeled using straightforward sinusoidal functions as described below:

$$F(z) = D \sin\left(m\frac{\pi z}{L}\right) \tag{1}$$

where D denotes the peak amplitude of the imperfection, m represents the number of half-waves, z is the longitudinal coordinate along the specimen, and L indicates the total length of the specimen. The amplitudes of these imperfections are chosen based on the experimental imperfection measurements [25] for the channel section.

The measured flexural imperfection about the weak axis (F_1/L) is found to be approximately 1/1580, whereas that about the strong axis (F_2/L) is minimal, around 1/4000. The initial twist (T/L) is roughly 0.6 degree per meter. The assumed global imperfection amplitudes adopted for analysis, therefore, are 1/1500

for weak-axis flexural imperfections and 0.6 degree per meter for the initial twist, whereas the strong-axis flexural imperfection is insignificant and thus omitted. The twisting imperfection is defined to be zero at the supports and to reach its peak value at mid-span.

The magnitudes of sectional imperfections are derived from the experimental data provided in Table 2. The imperfection magnitudes are formulated as a function of sectional slenderness (λ_s) and thickness, defined by the relation S = k × t × λ_s. Becque and Walker ([22,28]) recommended adopting a coefficient k = 0.3 to represent sectional imperfections. Meanwhile, experimental observations from the present study [25] indicated that *k* values range between 0.11–0.13 (for compression) and 0.18–0.27 (for bending) for local imperfections and 0.22–0.33 for distortional imperfections. The following amplitudes of sectional imperfections, therefore, are suggested and implemented as follows: (i) distortional imperfection S_2 = 0.3 × t × λ_d for both compression or bending, and (ii) local imperfection S_1 = 0.1 × t × λ_l in compression and 0.2 × t × λ_l in bending. Here, t represents the section thickness, while λ_l and λ_d denote the local and distortional slenderness parameters, respectively. These slenderness parameters are determined as follows: $\lambda_l = \sqrt{f_y/f_{ol}}$; $\lambda_d = \sqrt{f_y/f_{od}}$ where f_y is the yield strength; f_{ol} and f_{od} are the local and distortional buckling stresses, respectively.

The selection of half-wavelength numbers is influenced by the specific imperfection mode, the corresponding critical half-wavelengths associated with various buckling types for each section, and the overall specimen length. For global imperfections, a single half-wavelength is consistently applied, whereas for sectional imperfections, the number is determined according to the specimen length and the critical half-wavelengths obtained from the THIN-WALL-2 analysis [29].

The finite element modelling procedures for both beams and columns are thoroughly described and verified in detail in [25], including the material characteristics and geometric imperfections employed. Residual stresses were also incorporated in the FE models, as fully reported in Huynh [30]. The models for compression and bending are illustrated in Fig. 3. Then, the assumed geometric imperfections as described above mentioned are incorporated into the finite element models for compression and flexure, and this incorporation is thoroughly presented in Pham et al. [8].

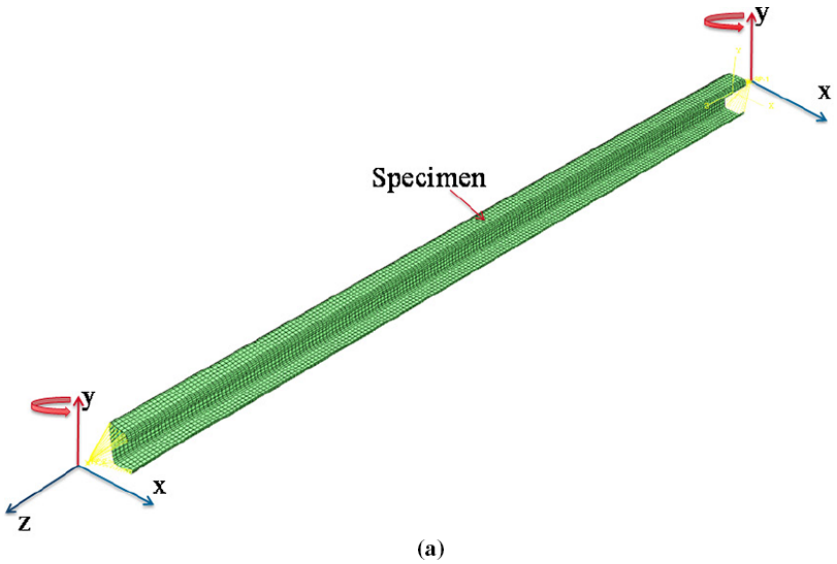

Figure 3: (Continued)

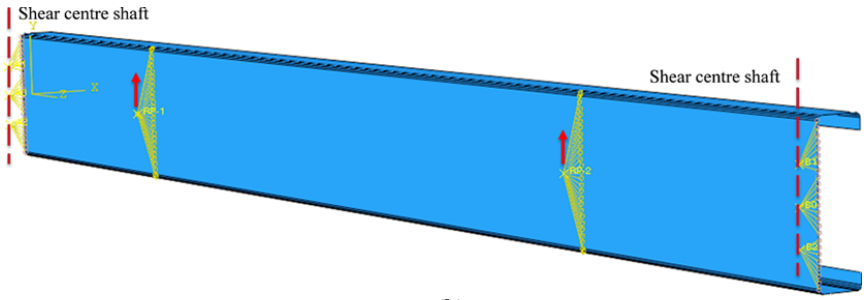

(b)

Figure 3: Finite element models for cold-formed aluminium alloy members. (**a**) Compression; (**b**) Flexure.

The comparisons between the test and numerical results are illustrated in Fig. 4 with a total of 30 compression samples and 20 flexural samples. If a point appears above the diagonal line, it indicates that the test strength exceeds the numerical prediction, and the opposite is true for points below the line. The mean and coefficient of variation (COV) derived from these comparisons are shown in Fig. 4, with values of (1.017, 0.029) for compression and (1.016, 0.048) for flexure.

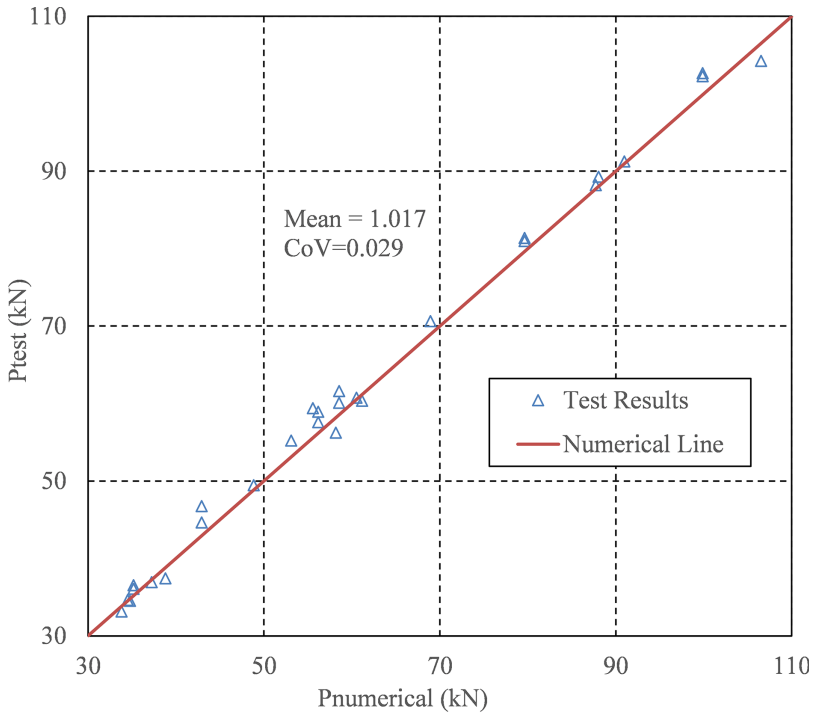

(a)

Figure 4: (Continued)

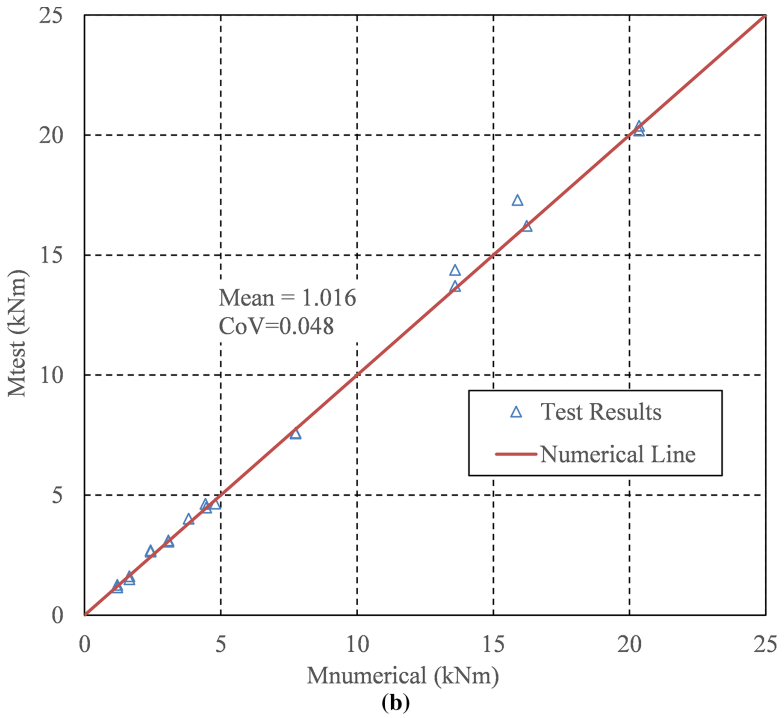

Figure 4: The comparisons between the test and numerical results. (**a**) Compression; (**b**) Flexure.

The results show that the simulations align closely with the experimental data. This confirms that the chosen geometric imperfections were appropriately defined for the parametric analyses. Hence, these representative imperfection models are adopted for subsequent numerical investigations of the channel sections, as outlined below:

- The flexural imperfection about the weak axis (F_1/L) is taken as 1/1500, while the imperfection about the strong axis (F_2/L) is neglected.
- The initial twist is assumed to be 0.6° per meter of length, starting from zero at the supports and reaching its maximum value at mid-span.
- The local imperfection (S_1) is defined as a function of sectional slenderness and thickness, with the coefficient k taken as 0.1 for compression and 0.2 for bending.
- The distortional imperfection (S_2) is represented using the k value of 0.3 for both compression and bending cases.

3 The Coefficient of Imperfections for Cold-Formed Aluminium Alloy Channel Members

Dubina and Ungureanu [12] demonstrated through numerical simulations that sectional imperfections have an insignificant influence on the moment strength and response of cold-formed steel members. In terms of cold-rolled aluminium structures, the geometric imperfection data remain limited. Following the discussion in [12], this study considers only global imperfections in the numerical simulations, as sectional imperfections were shown to have minimal influence.

3.1 The Selection of Finite Element Model for Column

Experimental and numerical findings reported in [25] revealed that flexural imperfections notably influence the capacities of cold-rolled aluminium alloy columns. Hence, this imperfection component has been included in this investigation for columns. The finite element model was constructed using the

ABAQUS software package [31] (see Fig. 3) and validated against an experimental program conducted at the University of Sydney, as reported in Pham et al. [32].

The section selected for this study is the C10030 profile, where "C" denotes a channel section, "100" represents a nominal depth of 100 mm, and "30" indicates a thickness of 3.0 mm. This section is taken from the commercial catalogue "Roll-formed Aluminium Purlin Solutions" published by BlueScope [2]. Its nominal dimensions are D = 105 mm, B = 60.5 mm, L = 16 mm, and t = 3.0 mm, with the nomenclature shown in Fig. 5.

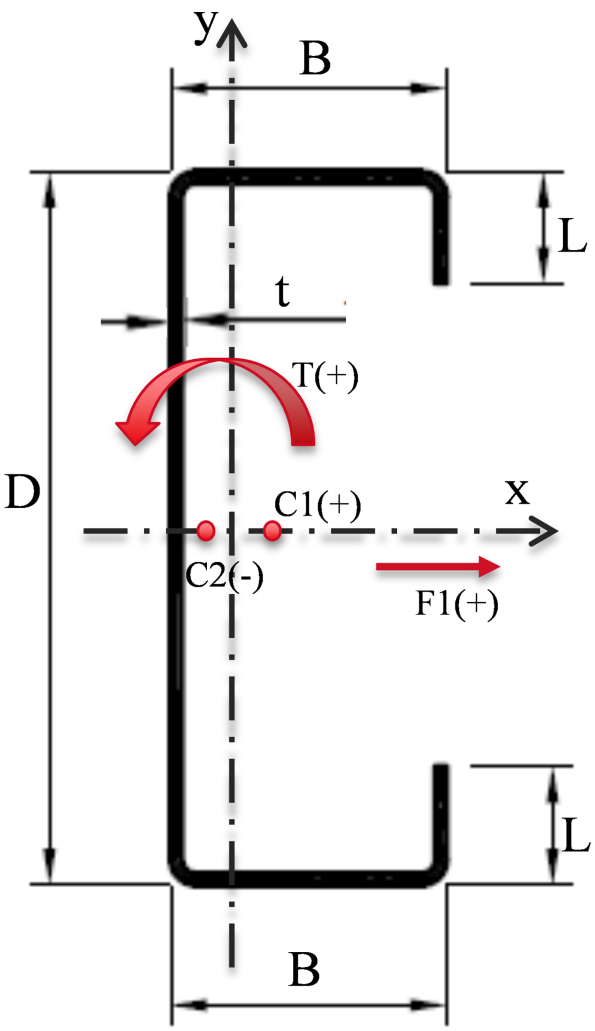

Figure 5: Nomenclature and the sign conventions.

Geometric imperfections were measured using the laser-scanner method described in Pham et al. [8], and these measured imperfections were incorporated directly into the simulation models, as detailed in the same reference. Following the approach in Pham [25], a nominal column eccentricity equal to 1/1500 of the member length was adopted for strength calculations. The weak-axis asymmetry of the channel section results in variations in the column capacities under different eccentricity sign conventions.

The sign conventions used in this study are shown in Fig. 5. A numerical study was performed on C10030 columns considering different eccentricity sign conventions to identify the most critical case as

shown in Fig. 6a. The results indicate that the positive eccentricity case, $C_1(+)$, is the critical condition and is therefore used in subsequent analyses.

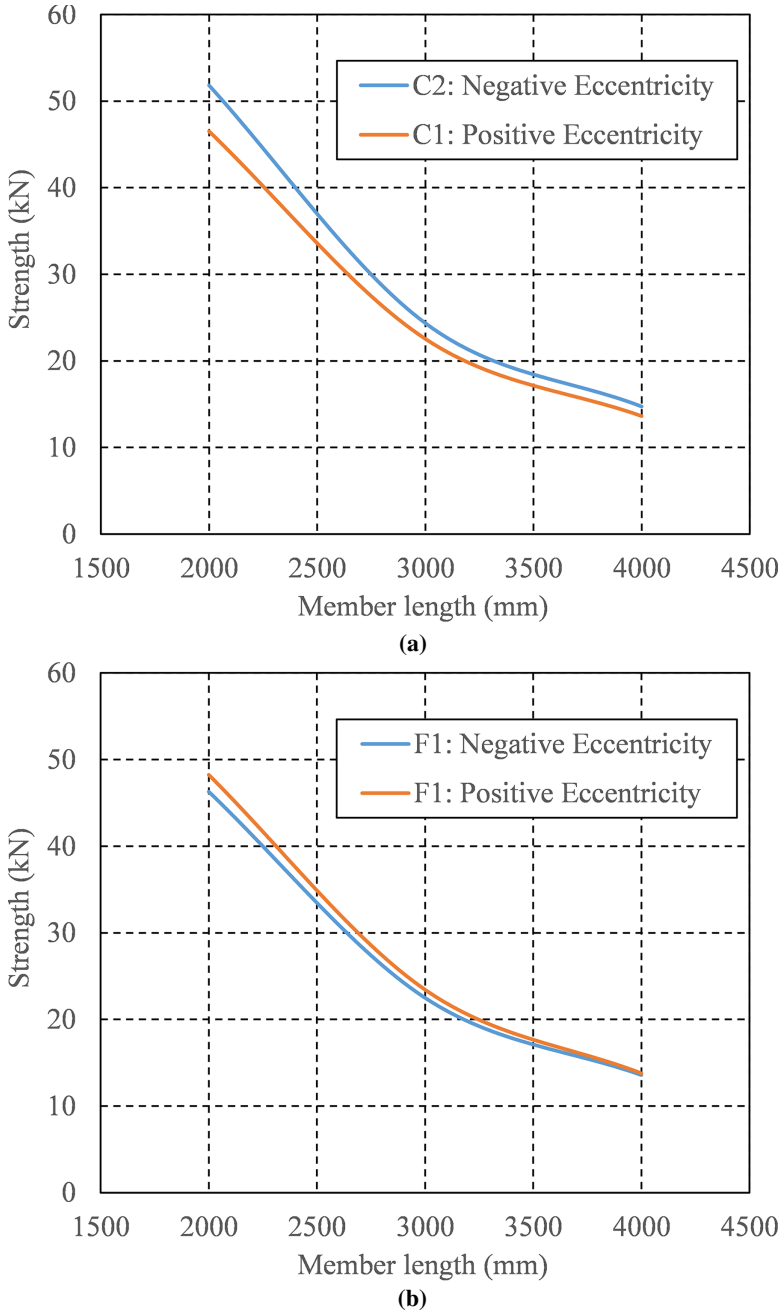

Figure 6: Numerical investigation for eccentricity and flexural imperfection sign. (**a**) Eccentricity position; (**b**) Flexural imperfection sign.

Flexural imperfections (F_1) are also examined, with sign conventions defined in Fig. 5. A parametric study is conducted to determine the most detrimental flexural imperfection, as illustrated in Fig. 6b. The results show that $F_1(-)$ leads to lower strengths and is therefore adopted for further investigation.

3.2 The Selection of Finite Element Model for Beam

The interaction between twisting and flexural imperfections and their combined impact on the strength and response of cold-rolled aluminium alloy channel beams has not yet been examined. Adopting the methodology proposed by Schillinger et al. [16], several global imperfection modes are introduced into the numerical models to identify the most critical buckling moment, which will serve as the basis for subsequent analyses.

In this study, the flexural imperfection components are combined with the twist imperfection to evaluate their influence on the reduction of beam strength and to identify the most critical cases for cold-rolled aluminium alloy beams. The magnitudes of these imperfections are defined using the mean values obtained from the measured data summarised in Section 2. For the analyses, the average amplitudes of F_1 and T are set to 1/1500 of the beam length and 0.6 degrees per meter, respectively. The F_2 component, with an average amplitude of 1/4084 of the beam length, is considered too small to have a meaningful effect and is therefore omitted. The investigation focuses on two global imperfection types—bow (F_1) and twist (T)—with their sign conventions illustrated in Fig. 5.

The cross-section examined in this study is the C10030 sections, where "C" denotes a channel profile, "100" represents the nominal depth in millimeters, and "30" indicates a thickness of 3.0 mm. The nonlinear finite element model employed in this work was based on the calibrated model developed in Pham et al. [10] which had been verified against experimental results, as shown in Fig. 3b. The beams are analysed under four-point bending with simple supports and free warping at both ends. The method for introducing global imperfections—F_1 and T—into the numerical model is described in detail in Pham et al. [8]. The outcomes of the investigation are presented in Fig. 7.

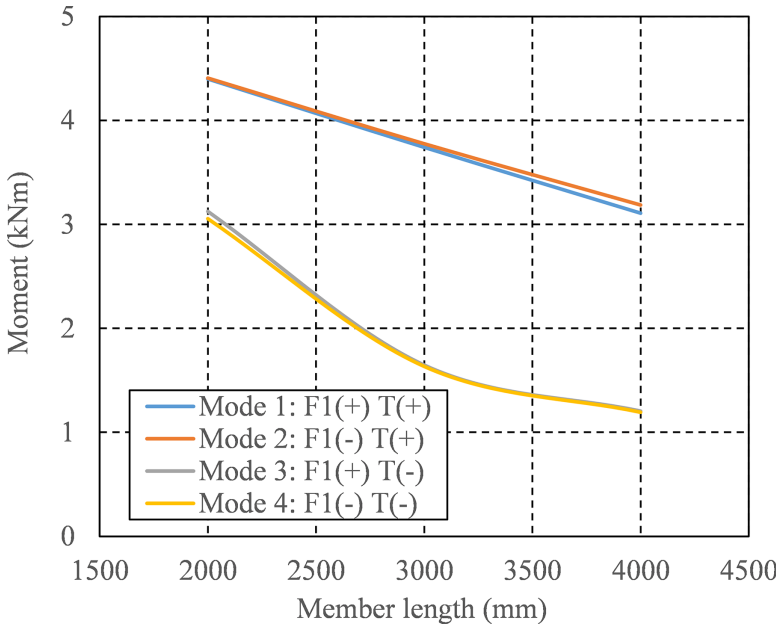

Figure 7: Numerical investigation for detrimental mode of combined imperfections.

The results show that the flexural imperfection component (F_1) has only a minor influence on beam strength, whereas twist imperfections (T) produce a pronounced effect. Among the investigated imperfection shapes, the combination $F_1(-)$ and T(−) leads to the lowest strengths. This imperfection mode, $F_1(-)$ and T(−), can therefore be regarded as the critical condition for subsequent studies. Furthermore, Fig. 7 clearly

demonstrates that variations in twist (T) considerably affect the strengths, while the influence of the flexural component is minimal. Twist (T), therefore, is selected as the primary variable for further analyses.

3.3 Determination of Coefficient of Imperfection V_I

This study aims to evaluate the coefficient of variation of the capacities of cold-rolled aluminium alloy beams and columns, considering the variability in the amplitudes of the twist imperfection component (T) and flexural imperfection (F_1). This coefficient is denoted as V_I in the present work. The T and F_1 amplitudes are randomly assigned based on the imperfection data reported by Pham [25]. To efficiently reduce the required number of random samples, the Latin Hypercube Sampling (LHS) technique [26] has been employed. The LHS technique is adopted in this study because it is a well-established variance reduction method that ensures efficient and representative coverage of the random variable space, allowing reliable statistical estimation with a relatively limited number of samples. The process for determining the coefficient V_I is outlined below:

- The measuring imperfection data reported in Pham [25] is employed to derive the probability density function for the imperfection components (F_1) and (T) using the EasyFit software package [33] with the mean and CoV as presented in Section 2.
- Randomised values of the F_1 and T components are then produced through the application of the Latin Hypercube Sampling (LHS) method [26].
- These generated imperfection amplitudes are introduced into the finite element (FE) models to assess the resulting member strengths. The obtained FE strength results form the basis for calculating the coefficient of variation, which quantifies the influence of global imperfections. This coefficient was subsequently adopted in the reliability assessment for the proposed design model.

In terms of compression, the compact C10030 section is selected for this study to eliminate the influence of interaction buckling modes. Three lengths from 1.5, 2.5, and 4.0 m are chosen to represent low, medium, and high slenderness ratios, respectively. The simulation models apply the critical imperfection combination, $F_1(-)$ with $C_1(+)$, to determine the strengths, which form the basis for calculating the proposed coefficient of variation (CoV).

Flexural imperfections (F_1) are treated as random variables generated according to the probability distribution of the measured data reported in Pham [25]. The Latin Hypercube sampling method is used to produce 30 random values of F_1 for each length, as shown by the probability density for the 2.5 m specimen in Fig. 8. This approach allows for an efficient representation of variability with a reduced number of samples [26].

The generated imperfection values were then incorporated into the numerical models to obtain compressive strength results. These results are represented as a probability density distribution in Fig. 9, yielding a CoV of 0.0196. Based on this analysis, a coefficient of variation of 0.02 is recommended for cold-formed aluminium alloy columns.

For the flexural study, the compact C15030 section is selected to prevent sectional buckling, with specimen lengths of 2.0, 4.0, and 6.0 m. In this designation, “C” denotes a channel section, “150” refers to the nominal depth of 150 mm, and “30” represents the thickness of 3.0 mm.

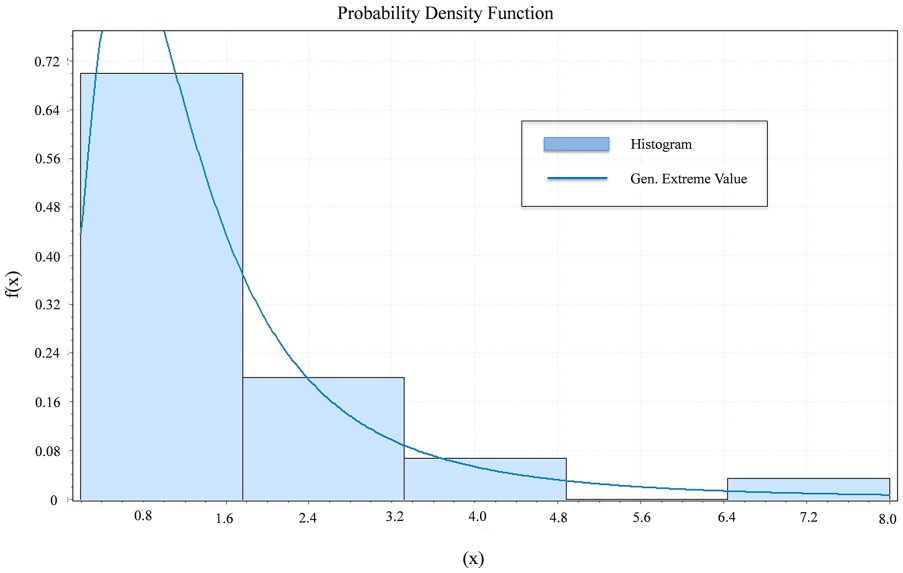

Figure 8: The radomised values of flexural imperfection (F_1) for C10030-2.5m.

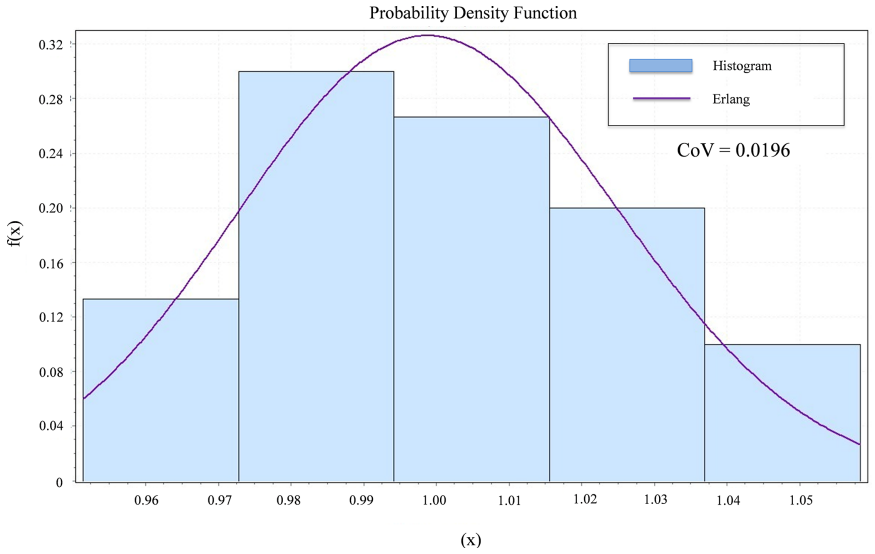

Figure 9: The probability density graph of cold-formed aluminium alloy columns.

The twist imperfection (T) is treated as a random variable, with its probability density derived from the experimental data reported in Pham [25]. Using the Latin Hypercube sampling method [26], 30 random values are generated for each specimen length. Fig. 10 illustrates the distribution of randomized twist values for C15030-6.0m sample. The flexural imperfection amplitude is set at 1/1500 of the beam length, as previously described.

Both global imperfections, F_1 and T, are incorporated into the finite element models for analysis. The obtained moments are plotted as a probability density distribution, shown in Fig. 11, yielding a CoV of 0.0298. Based on these results, a coefficient of variation (V_I) of 0.03 is proposed for cold-rolled aluminium alloy channel beams.

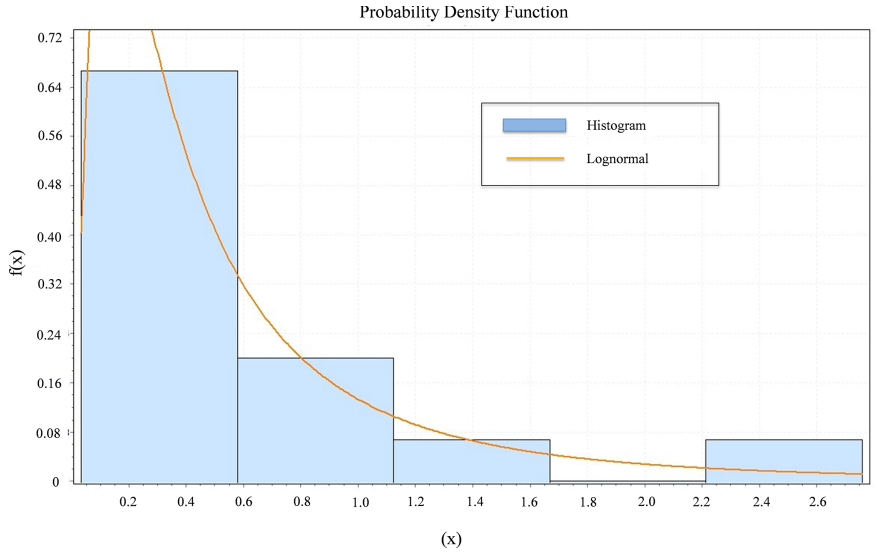

Figure 10: The randomised values of twist imperfection (T) for C15030-6.0m.

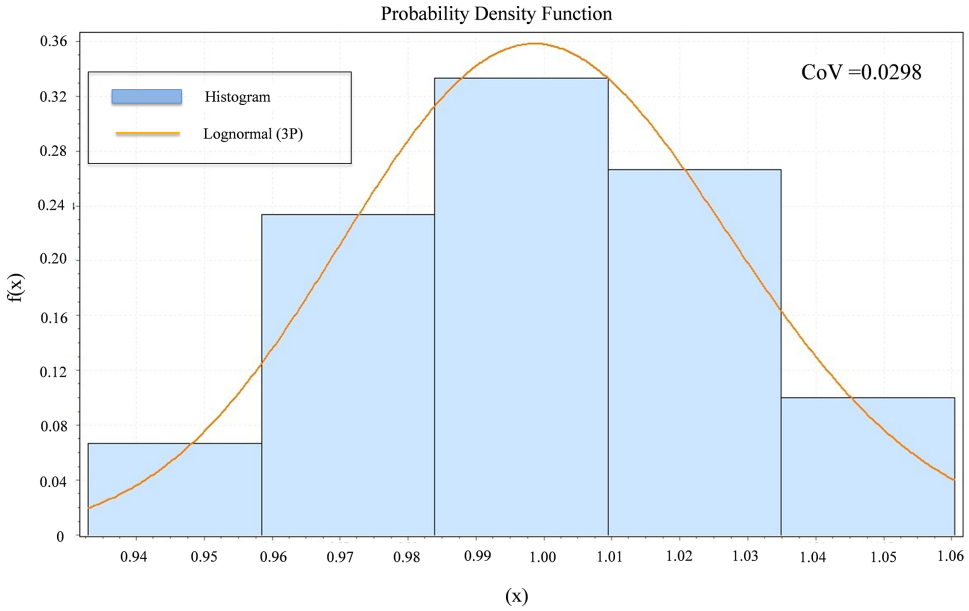

Figure 11: The probability density graph of cold-formed aluminium alloy beams.

The distributions in Figs. 8–11 were determined using the EasyFit software, which evaluates probability distributions based on statistical goodness-of-fit tests, including the Kolmogorov–Smirnov and Anderson–Darling statistics.

The calculated V_P mainly reflects modelling uncertainty and the discrepancy between the numerical strengths and the predicted strengths under these assumed average imperfection amplitudes. It does not represent the statistical variability of the geometric imperfections themselves. In contrast, the term V_I explicitly accounts for the variability associated with the magnitude and combination of geometric imperfections. Therefore, V_I is incorporated as an independent variance component to represent this additional source of uncertainty.

This V_I value will be incorporated into the reliability evaluation through the coefficient of variation of resistance (V_R) as expressed in Eq. (2). Then V_R will be used to determine the resistance factor (ϕ) as regulated in AA: 2015 [27]

$$V_R = \sqrt{V_M^2 + V_F^2 + C_n\left(V_P^2 + V_I^2\right)} \tag{2}$$

where the suggested coefficient V_I accounts for the influence of imperfections on the global buckling capacities of cold-rolled aluminium alloy channel members under compression or flexure; C_n is a correction factor; V_F, V_M and V_P correspond to the coefficients of variation associated with fabrication, material, and professional factors.

The reliability index for structural members is taken as $\beta = 2.5$ [27]. Based on this value, the resistance factor ϕ is determined using Eq. (3) with the load combination [1.2G + 1.6Q], where G represents the dead load and Q represents the live load. In this equation, M_m, F_m, and P_m represent the mean values associated with material properties, fabrication, and professional practice, while V_S and V_R correspond to the coefficients of variation for load effects and structural resistance. Further details are provided in the American Aluminum Specification [27].

$$\phi = \frac{1.5 M_m F_m P_m}{\exp\left(\beta\sqrt{V_R^2 + V_S^2}\right)} \tag{3}$$

4 Conclusions

This study presented a comprehensive analysis of geometric imperfections measured in cold-formed aluminium alloy channel members, compiled from previously published experimental data. The imperfection components were classified into global and local modes, and representative values were proposed as functions of section slenderness and thickness. These representative imperfection amplitudes were validated by comparing the ultimate strengths predicted from finite element analyses with available experimental results. The close agreement between numerical and experimental outcomes confirms the reliability of the proposed imperfection models.

The results highlight that the influence of geometric imperfections on the strength of cold-formed aluminium members is significant and should be properly accounted for in design and analysis. The coefficients of variation derived in this study provide a rational means of incorporating imperfection effects into reliability assessments and design formulations.

Acknowledgement: Not applicable.

Funding Statement: The authors received no specific funding.

Author Contributions: Hieu Nghia Hoang: Data curation, Investigation, Writing—original draft; Ngoc Hieu Pham: Conceptualization, Methodology, Supervision, Writing—review & editing; Quoc Anh Vu: Writing—review & editing; Trong Nghia Mai: Writing—review & editing. All authors reviewed and approved the final version of the manuscript.

Availability of Data and Materials: The dataset used and analyzed during the current study is available from the corresponding author [Ngoc Hieu Pham] upon reasonable request.

Ethics Approval: Not applicable.

Conflicts of Interest: The authors declare no conflicts of interest.

References

1. Szumigała M, Polus Ł. Applications of aluminium and concrete composite structures. Procedia Eng. 2015;108:544–9. doi:10.1016/j.proeng.2015.06.176.
2. BlueScope Lysaght. Permalite—aluminium roll-formed purlin solutions. Eagle Farm, Brisbane, QLD, Australia: Permalite Aluminium Building Solutions Pty Ltd.; 2015.
3. Mulligan GP. The influence of local buckling on the structural behavior of singly-symmetric cold-formed steel columns. Ithaca, NY, USA: Cornell University; 1983.
4. Dat DT, Pekoz TP. The strength of cold-formed steel columns. Ithaca, NY, USA: Cornell University; 1980.
5. Young B. The behaviour and design of cold-formed channel columns. Sydney, Australia: The University of Sydney; 1997.
6. Zhao X, Schafer BW. Measured geometric imperfections for Cee, Zee, and built-up cold-formed steel members. In: Proceedings of the Wei-Wen Yu International Specialty Conference on Cold-Formed Steel Structures; 2016 Nov 9–10; Baltimore, MD, USA. p. 73–8.
7. McAnallen LE, Padilla-Llano DA, Zhao X, Moen CD, Schafer BW, Easterling MR. Initial geometric imperfection measurement and characterization of cold-formed steel C-section structural members using 3D non-contact techniques. In: Proceedings of the Annual Stability Conference; 2014 Mar 25–28; Toronto, ON, Canada.
8. Pham NH, Pham CH, Rasmussen KJR. Incorporation of measured geometric imperfections into finite element models for cold-rolled aluminium sections. In: Proceedings of the 4th Congress International de Geotechnique-Ouvrages-Structures; 2017 Oct 26–27; Ho Chi Minh City, Vietnam. p. 161–71. doi:10.1007/978-981-10-6713-6_15.
9. Put BM, Pi YL, Trahair NS. Lateral buckling tests on cold-formed channel beams. J Struct Eng. 1999;125(5):532–9. doi:10.1061/(asce)0733-9445(1999)125:5(532).
10. Pham NH, Pham CH, Rasmussen KJR. Design of cold-rolled aluminium alloy channel beams subject to global buckling. Thin Walled Struct. 2022;180:109885. doi:10.1016/j.tws.2022.109885.
11. Pham NH, Pham CH, Rasmussen KJR. Experimental and numerical investigation of global buckling behaviour of cold-rolled aluminium alloy asymmetric section beams. Thin Walled Struct. 2025;217:113788. doi:10.1016/j.tws.2025.113788.
12. Dubina D, Ungureanu V. Effect of imperfections on numerical simulation of instability behaviour of cold-formed steel members. Thin Walled Struct. 2002;40(3):239–62. doi:10.1016/S0263-8231(01)00046-5.
13. Borges Dinis P, Camotim D, Silvestre N. FEM-based analysis of the local-plate/distortional mode interaction in cold-formed steel lipped channel columns. Comput Struct. 2007;85(19–20):1461–74. doi:10.1016/j.compstruc.2007.02.013.
14. Schafer BW, Zeinoddini VM. Impact of global flexural imperfections on the cold-formed steel column curve. In: Proceedings of the 19th International Specialty Conference on Recent Research and Development in Cold-Formed Steel Design and Construction; 2008 Oct 14–15; St. Louis, MO, USA. p. 81–95.
15. Rzeszut K, Garstecki A. Modeling of initial geometrical imperfections in stability analysis of thin-walled structures. J Theor Appl Mech. 2009;47(3):667–84.
16. Schillinger D, Papadopoulos V, Bischoff M, Papadrakakis M. Buckling analysis of imperfect I-section beam-columns with stochastic shell finite elements. Comput Mech. 2010;46(3):495–510. doi:10.1007/s00466-010-0488-y.
17. Crisan A, Ungureanu V, Dubina D. Behaviour of cold-formed steel perforated sections in compression: part 2—Numerical investigations and design considerations. Thin Walled Struct. 2012;61:97–105. doi:10.1016/j.tws.2012.07.013.
18. Gendy BL, Hanna MT. Effect of geometric imperfections on the ultimate moment capacity of cold-formed sigma-shape sections. HBRC J. 2017;13(2):163–70. doi:10.1016/j.hbrcj.2015.04.006.
19. Dou C, Pi YL. Effects of geometric imperfections on flexural buckling resistance of laterally braced columns. J Struct Eng. 2016;142(9):04016048. doi:10.1061/(asce)st.1943-541x.0001508.
20. Dinis PB, Young B, Camotim D. Local-distortional-global interaction in cold-formed steel lipped channel columns: behavior, strength and DSM design. In: SSRC Annual Stability Conference; 2016 Apr 12–15; Orlando, FL, USA. p. 654–87.

21. Pham NH. Numerical investigation of sectional buckling behaviors of cold-rolled aluminium alloy channel columns. Key Eng Mater. 2023;942:173–80. doi:10.4028/p-8lik6b.
22. Becque J. The interaction of local and overall buckling of cold-formed stainless steel columns. Sydney, Australia: The University of Sydney; 2008.
23. Yan J, Young B. Numerical investigation of channel columns with complex stiffeners: part I: test verification. Thin Walled Struct. 2004;42(6):883–93. doi:10.1016/j.tws.2003.12.002.
24. Young B, Yan J. Numerical investigation of channel columns with complex stiffeners: part II: parametric study and design. Thin Walled Struct. 2004;42(6):895–909. doi:10.1016/j.tws.2004.01.004.
25. Pham NH. Strength and behaviour of cold-rolled aluminium members. Sydney, Australia: The University of Sydney; 2019.
26. McKay MD, Beckman RJ, Conover WJ. A comparison of three methods for selecting values of input variables in the analysis of output from a computer code. Technometrics. 2000;42(1):55–61. doi:10.1080/00401706.2000.10485979.
27. Aluminum Association. Aluminum design manual. Washington, DC, USA: Aluminum Association; 2020.
28. Walker AC. Design and analysis of cold-formed sections. London, UK: International Textbook Company Ltd.; 1975.
29. Nguyen VV, Hancock GJ, Pham CH. Development of thin-wall-2 for buckling analysis of thin-walled sections under generalised loading. In: Proceedings of the 8th International Conference on Advances in Steel Structures; 2015 Jul 22–24; Lisbon, Portugal.
30. Huynh LAT. Strength and behaviour of cold-rolled aluminium sections. Sydney, Australia: The University of Sydney; 2019.
31. Dassault Systemes Simulia Corp. ABAQUS/CAE user's manual. Providence, RI, USA: Dassault Systemes Simulia Corp.; 2014 [cited 2026 Jan 1]. Available from: http://130.149.89.49:2080/v2016/pdf_books/CAE.pdf.
32. Pham NH, Pham CH, Rasmussen KJR. Member capacity of cold-rolled aluminium alloy channel columns—Part II: numerical investigation and design. Thin Walled Struct. 2024;200:111960. doi:10.1016/j.tws.2024.111960.
33. Mathforum.org. EasyFit: distribution-fitting software. Chicago, IL, USA: Park City Mathematics Institute; 1994 [cited 2026 Jan 1]. Available from: https://easyfit.informer.com/.